

## <sup>13</sup>CHD<sub>2</sub> Methyl Group Probes of Millisecond Time Scale Exchange in Proteins by <sup>1</sup>H Relaxation Dispersion: An Application to Proteasome Gating Residue Dynamics

Andrew J. Baldwin, Tomasz L. Religa, D. Flemming Hansen, Guillaume Bouvignies, and Lewis E. Kay\*

Departments of Molecular Genetics, Biochemistry and Chemistry, The University of Toronto, Toronto, Ontario, M5S 1A8, Canada

Received May 26, 2010; E-mail: Kay@pound.med.utoronto.ca

**Abstract:** A pulse scheme is presented for quantifying millisecond time scale chemical exchange processes in proteins by measuring <sup>1</sup>H CPMG relaxation dispersion profiles of <sup>13</sup>CHD<sub>2</sub> methyl groups. The use of <sup>13</sup>CHD<sub>2</sub> isotopomers for <sup>1</sup>H methyl dispersion experiments eliminates problems with interconversion between differentially relaxing proton transitions that complicate the extraction of accurate exchange parameters when <sup>13</sup>CH<sub>3</sub> probes are used. Good agreement is demonstrated between extracted chemical shift differences from fits of dispersion profiles and the corresponding differences measured independently on a model exchanging system, validating the experiment. The methodology is applied to the gating residues of the *T. acidophilium* proteasome that are shown to undergo extensive motion on the millisecond time scale.

Over the past decade the utility of methyl groups in NMR studies of protein structure and dynamics has been clearly demonstrated.<sup>1–3</sup> The success of methyls as macromolecular probes arises, in part, from their inherent spin physics that leads to classes of both slowly and rapidly relaxing transitions.<sup>4,5</sup> The development of simple experiments that isolate these slow/fast relaxing <sup>13</sup>CH<sub>3</sub> transitions and prevent them from mixing has played an important role in improving the sensitivity and resolution of <sup>13</sup>C–<sup>1</sup>H methyl correlation maps,<sup>5</sup> thereby facilitating studies of protein systems with aggregate molecular weights in the hundreds of kDa.<sup>3,6–8</sup> Isolation of the differentially relaxing methyl coherences can also be critical to the accuracy of measured relaxation rates that probe motional processes in proteins, as illustrated by the <sup>1</sup>H Carr–Purcell–Meiboom–Gill (CPMG) relaxation dispersion method that quantifies millisecond (ms) time scale dynamics.<sup>9</sup> In this experiment a variable number of <sup>1</sup>H refocusing pulses are applied during a CPMG element to modulate the effective methyl <sup>1</sup>H-transverse relaxation rate,  $R_{2,\text{eff}}$ , from which the thermodynamic and kinetic parameters that describe the exchange process can be obtained. However, (unavoidable) imperfections in the refocusing pulses lead to the interconversion of slow/fast relaxing <sup>1</sup>H coherences, producing significant artifacts in dispersion data sets that complicate extraction of robust exchange parameters.<sup>10</sup> We have recently developed a pulse scheme that suppresses these artifacts but at the expense of an approximate 10-fold reduction in sensitivity relative to a simple <sup>13</sup>C,<sup>1</sup>H HMQC spectrum.<sup>11</sup> Clearly such sensitivity losses are unacceptable in studies involving high molecular weight proteins where signal-to-noise (*s/n*) is a major concern.

The simplest way of preventing the interconversion between differentially relaxing methyl <sup>1</sup>H transitions resulting from pulse imperfections during the CPMG pulse train is to perform experiments using a ‘simplified’ methyl spin system with only a single

proton, such as would be provided by a <sup>13</sup>CHD<sub>2</sub> probe. We have recently shown that the *s/n* of <sup>13</sup>C,<sup>1</sup>H methyl correlations in spectra of U-[<sup>2</sup>H], Ile-[<sup>13</sup>CHD<sub>2</sub> δ1], Leu,Val-[<sup>13</sup>CHD<sub>2</sub>,<sup>13</sup>CHD<sub>2</sub>]-labeled half proteasome (360 kDa) is 1.5–2-fold lower than that for data sets measured on U-[<sup>2</sup>H], Ile-[<sup>13</sup>CH<sub>3</sub> δ1], Leu,Val-[<sup>13</sup>CH<sub>3</sub>,<sup>12</sup>CD<sub>3</sub>] samples.<sup>12</sup> Thus, while there are sensitivity losses associated with <sup>13</sup>CHD<sub>2</sub>- compared to <sup>13</sup>CH<sub>3</sub>-labeling, the losses are not expected to be prohibitive and are certainly much less extreme than the factor of 10 mentioned above. In what follows, a methyl-based <sup>1</sup>H CPMG pulse scheme for quantifying ms exchange dynamics in proteins is presented that exploits the simplicity of the <sup>13</sup>CHD<sub>2</sub> probe. The utility of the approach is established through cross-validation using a protein–ligand exchanging system that has been well characterized previously,<sup>13</sup> and an application to quantifying ms time-scale exchange in the *T. acidophilium* proteasome is presented.

Figure 1 shows the pulse scheme that has been developed for recording <sup>1</sup>H CPMG dispersion profiles of <sup>13</sup>CHD<sub>2</sub> methyl probes in highly deuterated proteins. Central to the experiment is the constant-time CPMG element<sup>14</sup> between points *a* and *b*, during which time <sup>1</sup>H transverse magnetization evolves as a function of  $\nu_{\text{CPMG}} = 1/(4\tau_{\text{CP}})$ , where  $\tau_{\text{CP}}$  is the duration between successive 180° refocusing pulses. The constant-time relaxation period,  $T_{\text{relax}}$ , is divided into two equal elements, separated by a 180° pulse of phase  $\phi_2$  that is applied along an axis orthogonal to the CPMG pulses. As described previously, this central pulse leads to a refocusing of artifacts that are produced from pulse imperfections and resonance offset effects during the CPMG element.<sup>15</sup> After the delay  $T_{\text{relax}}$ , <sup>13</sup>C chemical shift evolution is recorded with preservation of both cosine and sine modulated  $t_1$  components<sup>16,17</sup> that are subsequently transferred to <sup>1</sup>H for observation ( $t_2$ ) using a planar-TOCSY mixing scheme<sup>18,19</sup> that minimizes exchange mediated relaxation losses.  $R_{2,\text{eff}}(\nu_{\text{CPMG}})$  values are calculated as  $(1/T_{\text{relax}}) \ln(I/I_0)$  where  $I$  and  $I_0$  are the intensities of peaks in spectra recorded with and without the CPMG element,<sup>14</sup> respectively.

$R_{2,\text{eff}}(\nu_{\text{CPMG}})$  rates can be highly sensitive to chemical exchange. A second process, unrelated to chemical exchange, results from the evolution of <sup>1</sup>H magnetization due to the one-bond <sup>1</sup>H–<sup>13</sup>C scalar coupling,  $J_{\text{CH}}$ , that will also modulate  $R_{2,\text{eff}}$ . Starting from point *a* of Figure 1 the magnetization of interest,  $2I_yC_z$  ( $A_i$  is the  $i \in \{x,y,z\}$  component of  $A$  magnetization), interconverts with  $I_x$  as a function of  $\tau_{\text{CP}}$ . The imbalance in relaxation rates between in-phase ( $I_x$ ) and antiphase ( $2I_yC_z$ ) <sup>1</sup>H magnetization can create artificial dispersion profiles<sup>20</sup> that can be calculated as<sup>21</sup>

$$R_{2,\text{eff}}(\tau_{\text{CP}}) = R_{2,A} + 0.5(R_{2,I} - R_{2,A}) \left( 1 - \frac{\sin(2\pi J_{\text{CH}}\tau_{\text{CP}})}{2\pi J_{\text{CH}}\tau_{\text{CP}}} \right) \quad (1)$$

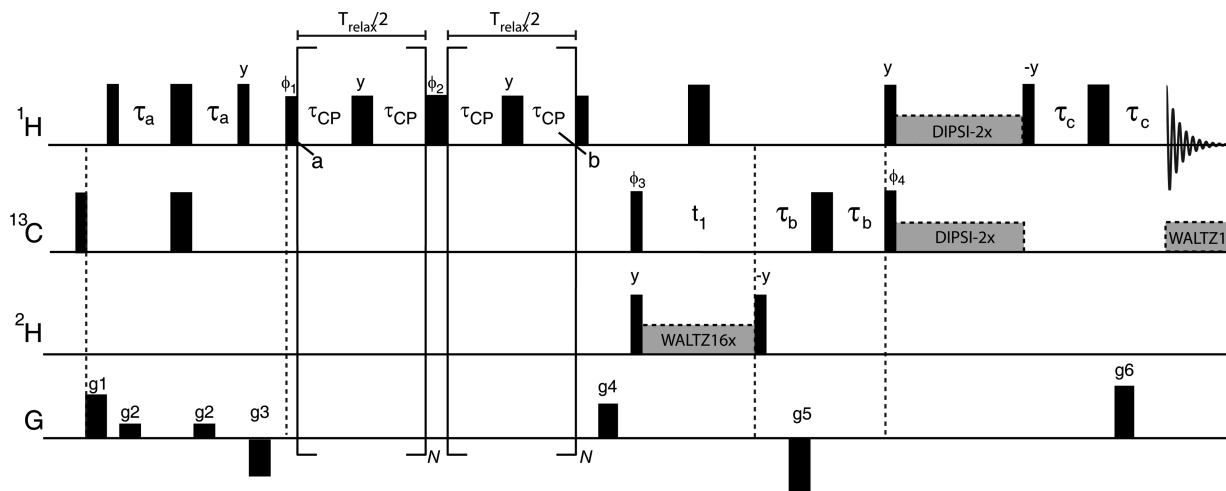


**Figure 1.** Pulse scheme of the enhanced sensitivity methyl  $^1\text{H}$  CPMG dispersion experiment for studies of ms time scale exchange in  $^{13}\text{CHD}_2$ -labeled proteins. All pulses are applied along the  $x$ -axis unless indicated otherwise. All  $^1\text{H}$  and  $^{13}\text{C}$  pulses are at the highest possible power levels, with the exception of the  $^1\text{H}$  pulses during the constant-time CPMG element, including the flanking  $90^\circ$  pulses, that are applied with a field strength of 10 kHz. A pair of 8kHz  $^1\text{H}/^{13}\text{C}$  DIPSII-2x elements<sup>27</sup> are used to effect heteronuclear cross-polarization (duration of  $\sim 1/J_{\text{HC}}$ ), and  $^{13}\text{C}$  decoupling during acquisition is achieved with a 2 kHz WALTZ-16 field.<sup>28</sup> 1.5 kHz  $^2\text{H}$  pulses flank the 550 Hz  $^2\text{H}$  decoupling element. The values of  $\tau_a$ ,  $\tau_b$ , and  $\tau_c$  are set to 2 ms, 550  $\mu\text{s}$ , and 575  $\mu\text{s}$ , respectively. The delay  $T_{\text{relax}}$  is set for  $\sim 50\%$  intensity reduction relative to  $T_{\text{relax}} = 0$ .  $N$  is any integer. The phase cycle employed is as follows:  $\phi_1 = (x, -x)$ ,  $\phi_2 = 2(x), 2(-x), \phi_3 = 2(x), 2(-x)$ ,  $\phi_4 = y$ , rec. =  $x, 2(-x), x$ . Quadrature in  $F_1$  is obtained by recording a pair of data sets for each  $t_1$  value corresponding to  $(g_5, \phi_4)$  and  $(-g_5, -\phi_4)$ . Durations and strengths of the  $z$ -axis gradient pulses are (ms, G/cm):  $g_1 = (1.0, 40)$ ,  $g_2 = (0.6, 16)$ ,  $g_3 = (1.0, -24)$ ,  $g_4 = (0.3, 30)$ ,  $g_5 = (0.25, -60)$ ,  $g_6 = (0.125, 29.64)$ .

in the limit  $2\pi J_{\text{CH}} \gg R_{2,I} - R_{2,A}$  where  $R_{2,I}$  ( $R_{2,A}$ ) is the transverse relaxation rate of in-phase (antiphase) magnetization. To excellent approximation<sup>22</sup> (see Supporting Information, SI)

$$R_{2,I} - R_{2,A} = \left( \frac{\mu_0}{4\pi} \right) \frac{23\gamma_{\text{H}}^2 r_{\text{HC}}^2 \hbar^2}{10r_{\text{HC}}^6} J(\omega_{\text{C}}) \quad (2)$$

where  $\gamma_j$  is the gyromagnetic ratio of spin  $j$ ,  $r_{\text{HC}}$  is the intramethyl  $^1\text{H}$ – $^{13}\text{C}$  distance, and  $J(\omega_{\text{C}})$  is the spectral density function describing the methyl group dynamics evaluated at a frequency of  $\omega_{\text{C}}$ . Loria et al.<sup>20</sup> insert an element in the center of the CPMG train that eliminates the  $\tau_{\text{CP}}$  dependence on  $R_{2,\text{eff}}$  from the relaxation mismatch so that  $R_{2,\text{eff}}(\tau_{\text{CP}}) = 0.5(R_{2,I} + R_{2,A})$ . We have chosen not to use such a scheme here since (i) it then becomes possible to record dispersions with  $\nu_{\text{CPMG}}$  values that are half as large as would be otherwise possible, an important consideration in cases where exchange rates are small<sup>15</sup> (on the order of 100–200  $\text{s}^{-1}$ ); (ii)  $R_{2,I} - R_{2,A}$  values are typically very small ( $< 0.5 \text{ s}^{-1}$ , on average, in the systems studied here) so that errors in dispersion profiles are less than 0.3  $\text{s}^{-1}$ , well within experimental noise for most applications (see below); (iii) nonzero values of  $R_{2,I} - R_{2,A}$  can be explicitly taken into account in fits of dispersion profiles using an exchange matrix that includes both  $^{13}\text{C}$  and  $^1\text{H}$  spins (software can be downloaded at <http://pound.med.utoronto.ca/software>).

In order to evaluate the methodology we have first recorded  $^1\text{H}$  dispersion profiles on a U-[ $^2\text{H}$ ], Ile-[ $^{13}\text{CHD}_2$   $\delta 1$ ], Leu, Val-[ $^{13}\text{CHD}_2$ ,  $^{13}\text{CHD}_2$ ]-protein (abp1p SH3 domain) – U-[ $^2\text{H}$ ] ligand (Ark1p peptide) exchanging system that has been described in detail previously<sup>13</sup> and for which chemical shifts of the free and bound protein states are already known.<sup>23</sup> A comparison of the extracted shift differences from fits of CPMG dispersion profiles,  $\Delta\omega_{\text{H}}(\text{CPMG})$ , with the corresponding values obtained directly from analyses of spectra of peptide free and fully bound protein,  $\Delta\omega_{\text{H}}(\text{direct})$ , provides a sensitive test of the methodology. Figure 2a plots  $R_{2,\text{eff}}(\nu_{\text{CPMG}})$  vs  $\nu_{\text{CPMG}}$  for Ile26H $\delta 1$  and Leu49H $\delta 1$  recorded at 600 and 800 MHz, at 25  $^\circ\text{C}$  (i) and 5  $^\circ\text{C}$  (ii). Dispersion profiles are small; of the 18 Ile, Leu, Val methyl groups in the abp1p SH3

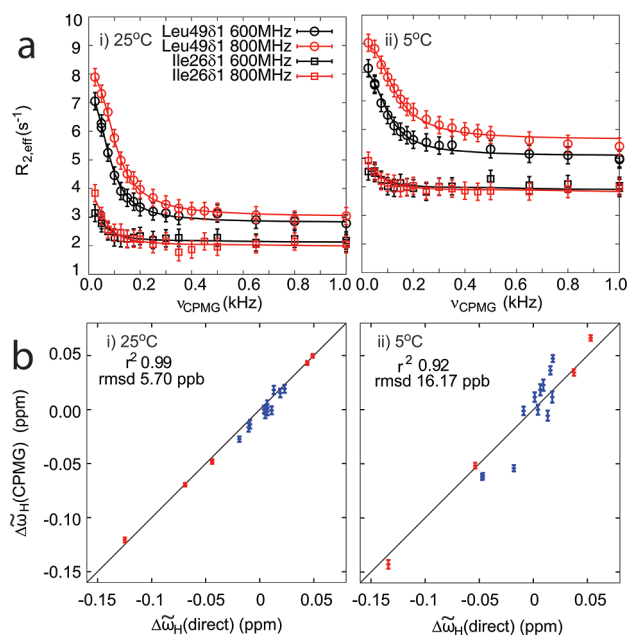


**Figure 2.** (a)  $^1\text{H}$  methyl relaxation dispersion profiles for Ile26H $\delta 1$  and Leu49H $\delta 1$  recorded at 600 (black) and 800 (red) MHz, at 25  $^\circ\text{C}$  (i) and 5  $^\circ\text{C}$  (ii). Continuous lines are the fits to the data (circles for Leu49/squares for Ile26) assuming a model of two-site exchange. (b) Correlation of  $\Delta\omega_{\text{H}}(\text{CPMG})$  vs  $\Delta\omega_{\text{H}}(\text{direct})$  ( $\Delta\omega_{\text{H}} = \omega_{\text{Apo}} - \omega_{\text{Holo}}$ ). Red (blue) points are those for which the signs of  $\Delta\omega_{\text{H}}(\text{CPMG})$  were (were not) obtained by the method of Skrynnikov et al.<sup>29</sup> In cases where signs could not be elucidated using this approach they were obtained directly from spectra of apo and fully ligand bound protein.

domain the largest  $R_{2,\text{ex}}(\nu_{\text{CPMG}})$  curve is from Leu49H $\delta 1$ , while the profile for Ile26H $\delta 1$  is more typical with  $R_{2,\text{ex}} = R_{2,\text{eff}}(\nu_{\text{CPMG}} = 25 \text{ Hz}) - R_{2,\text{eff}}(\nu_{\text{CPMG}} = 1 \text{ kHz}) \approx 1 \text{ s}^{-1}$ , which is fit with a very small  $\Delta\omega_{\text{H}}$  value (0.04 ppm). Nevertheless, good fits (continuous lines) to the data (circles/rectangles) are obtained when all of the dispersion curves at a given temperature are fit simultaneously to a model of two-site exchange that has been described previously.<sup>13</sup>

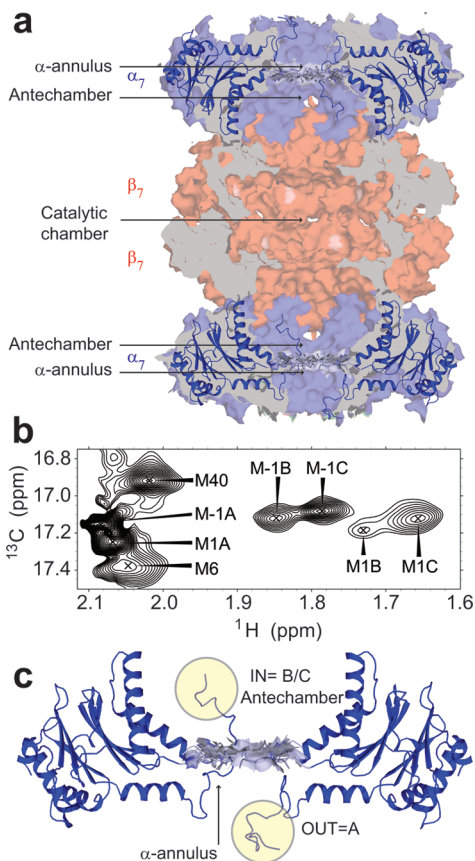


**Figure 3.** (a) Space filling cross-sectional side-view representation of the 20S CP proteasome ( $\alpha_7\beta_7\beta_7\alpha_7$ ) from *Thermoplasma acidophilum*, showing the relative positions of the  $\alpha$ -annulus, the antechambers and the catalytic chamber.<sup>30</sup> (b)  $^{13}\text{C}$ ,  $^1\text{H}$  HMQC correlation map of U- $^{2}\text{H}$ , Met- $^{13}\text{CH}_3$   $\alpha_7$ , 50 °C. Correlations from Met-1/Met1 are labeled A, B, and C. (c) Structure showing two of the seven  $\alpha$  subunits of  $\alpha_7$  with gating termini either 'out' or 'in' the lumen of the proteasome barrel. Peaks labeled A and B/C in the spectrum derive from the 'out' and 'in' conformations, respectively.<sup>25</sup>

Figure 2b correlates  $\Delta\omega_{\text{H}}(\text{CPMG})$  vs  $\Delta\omega_{\text{H}}(\text{direct})$ , and the good agreement is apparent. The slightly poorer correlation for the data

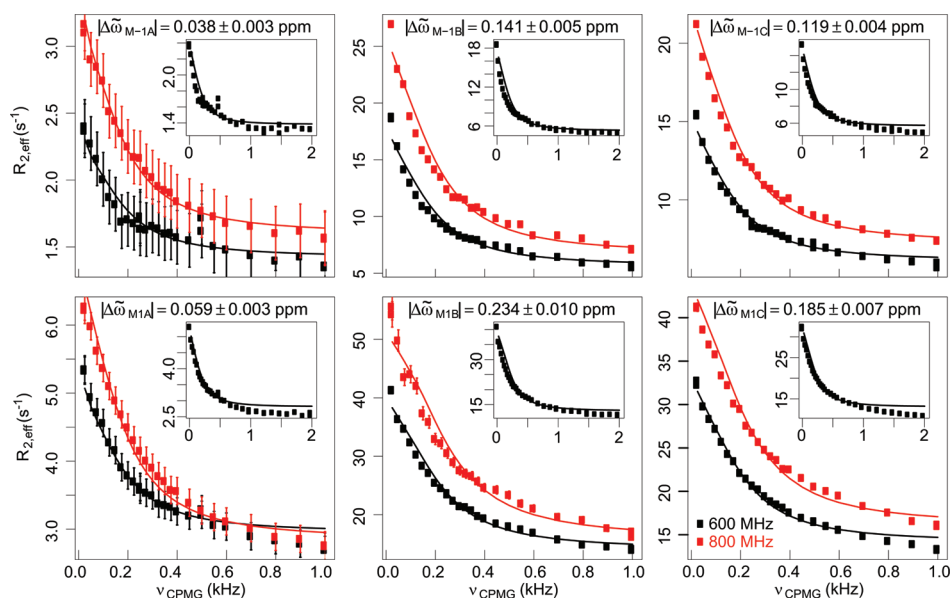


**Figure 4.**  $^1\text{H}$  methyl relaxation dispersion profiles for M-1 and M1 (states A, B, and C) of  $\alpha_7$  recorded at 600 (black) and 800 MHz (red), 50 °C, and fit to a model of two-site chemical exchange. Values of  $|\Delta\tilde{\omega}|$  extracted from fits are listed.  $^1\text{H}$  dispersion profiles recorded to 2 kHz (600 MHz) are illustrated in insets.

recorded at 5 °C reflects the fact that smaller dispersion profiles are measured at the lower temperature. Although the plotted correlations are based on an analysis that includes residue specific  $R_{2,I} - R_{2,A}$  values (see SI), only small changes in  $r^2$  and rmsd are noted when  $R_{2,I} - R_{2,A} = 0$  is assumed ( $r^2 = 0.97$ , rmsd = 8.0 ppb vs  $r^2 = 0.99$ , rmsd = 5.7 ppb for the 25 °C data). In general, it is not anticipated that the in-balance in relaxation rates will lead to measurable errors in extracted exchange parameters, especially in cases where amplitudes of dispersion profiles are larger than 2–3  $\text{s}^{-1}$ . This effect will become even smaller as applications extend to larger proteins since  $J(\omega_C)$  decreases with molecular size (see eq 2).

Satisfied that the methodology is robust, we focus now on an application probing ms time scale dynamics in the gating residues of the 20S core particle proteasome (20S CP). The 20S CP is a barrel-like structure comprised of four heptameric rings,<sup>24</sup> Figure 3a, that are arranged one on top of the other, and in the *T. acidophilum* version that we study here each of the rings consists of identical  $\alpha$ - ( $\beta$ -) subunits (referred to as  $\alpha_7$ ,  $\beta_7$ ) to form an  $\alpha_7\beta_7\beta_7\alpha_7$  structure. The N-terminal 10–15 residues of each  $\alpha$  subunit play a critical role in preventing intrinsically disordered or partially disordered proteins from inadvertently entering the proteasome chamber and undergoing untimely degradation (gating). Previous studies by our group have provided evidence of ms dynamics in the gate region.<sup>6,24,25</sup> For example, the absence of  $^{15}\text{N}$ – $^1\text{H}^{\text{N}}$  correlations from amides localized to regions surrounding the gating residues in spectra of  $\alpha_7$  (180 kDa) and the low intensity of  $^{13}\text{C}$ – $^1\text{H}$  methyl correlations derived from Ile, Leu, and Val probes in  $\alpha_7\alpha_7$  that are in the vicinity of the gate are consistent with the presence of ms time-scale motions.

In a recent study we have quantified the structural and motional properties of the proteasome gates using a highly deuterated Met- $^{13}\text{CH}_3$  sample of  $\alpha_7$  (ref 25). Methionine residues are often highly flexible, and it was anticipated that the high degree of mobility would at least partially 'average away' exchange contributions to peak line widths, permitting measurement of high quality data sets. A  $^{13}\text{C}$ ,  $^1\text{H}$  correlation plot of Met-labeled  $\alpha_7$  is presented in Figure 3b, illustrating that excellent spectra can be obtained with this labeling scheme and, of interest, that the number of observed

correlations is larger than the expected 5 (Met-1, Met1, Met6, Met40, Met120) (ref 25). We have shown previously that the extra peaks result from the fact that each of the gating termini can exist in three discrete states, Figure 3c, one of which is outside the lumen of the barrel,<sup>25</sup> and the correlations labeled 'A' in Figure 3b for Met-1 and Met1 are derived from this state. The gating residues for the other two conformers are inside the lumen (peaks 'B'/'C' in Figure 3b). These results have important implications for function since by extending into the 20S CP the termini decrease the surface area of the  $\alpha$ -annulus that forms the gateway for substrates to enter the proteasome, thereby 'closing the gate'. Moreover, the gates are highly dynamic over a broad spectrum of time scales. They interconvert between 'in' and 'out' with lifetimes of each state on the order of several seconds as established by magnetization exchange spectroscopy, experience a wide range of ps–ns motions, and, as described above, undergo ms fluctuations.<sup>25</sup> The presence of high intensity peaks for Met-1, Met1, and Met6, localized to the gating region of each subunit, suggests that unlike for amides and Ile, Leu, and Val methyl probes of the gates that give rise to spectra of poor quality, the Met gate residues can be used to accurately quantify ms exchange processes.

A sample of highly deuterated Met-[<sup>13</sup>CHD<sub>2</sub>]  $\alpha_7$  was prepared by addition of Met-[<sup>13</sup>CHD<sub>2</sub>] (other positions on the Met precursor are protonated) to protein expression media prior to induction, as has been described previously.<sup>25</sup> Dispersion curves were subsequently recorded at 600 (black) and 800 (red) MHz, 50 °C, using the scheme of Figure 1 and all profiles from M-1, M1, and M6 fit simultaneously to a model of two-site chemical exchange (solid lines). Values of  $p_B = 6.0\%$  (population of the minor state) and  $k_{ex} = 1030 \text{ s}^{-1}$  (sum of forward and reverse exchange rates) were obtained, along with  $|\Delta\omega|$  values for each residue that are shown in the panels of Figure 4. Although the fits are reasonable, for a number of correlations it is clear that a process more complex than two-state is likely to be operative (see insets that extend to  $\nu_{\text{CPMG}}$  values of 2 kHz). Fits of dispersion profiles were also performed therefore by analyzing curves from (i) the 'in' and 'out' states independently or from (ii) states A, B, and C independently. Values of shift differences were very similar to those obtained from the global fit, with  $p_B$  and  $k_{ex}$  ranges of 5–10% and 900–1700  $\text{s}^{-1}$ , respectively. Extraction of robust exchange parameters/shifts was not possible from independent fits of profiles from state A since the smaller  $\Delta\omega$  values place the exchange time scale close to the fast regime. Presently we have not elucidated the structural properties of the gating residues in the excited state. However, it is clear that there are significant chemical shift differences relative to the ground state, in particular for conformers B/C, suggesting substantial changes in the environments of the methyl probes between the different exchanging conformers. Of interest, in this application Met <sup>13</sup>C methyl dispersion profiles are significantly smaller than the corresponding curves for <sup>1</sup>H (maximum dispersion sizes of 3–4  $\text{s}^{-1}$ ). This emphasizes the complementarity between previously developed <sup>13</sup>C dispersion schemes for quantifying methyl exchange<sup>26</sup> and the <sup>1</sup>H based method proposed here.

In summary, a sensitive pulse scheme has been presented for studying ms time-scale exchange using <sup>13</sup>CHD<sub>2</sub> methyl probes in proteins. The accuracy of the methodology has been established by comparing chemical shift differences extracted from fits of dispersion profiles with the corresponding values measured on a system for which it is possible to record high quality spectra of both exchanging states through the manipulation of sample condi-

tions. An application to the  $\alpha_7$  ring of the proteasome shows that the gating residues undergo ms time scale exchange that is reasonably well modeled by assuming that the dominant conformer exchanges with a low populated state at a rate of  $\sim 1000 \text{ s}^{-1}$ . Structural differences in gating residues between ground and excited state conformers are likely to be significant, especially for the 'in' conformers, where Met <sup>1</sup>H chemical shift differences between the interconverting conformations are large. The <sup>1</sup>H CPMG experiment described here extends the utility of methyl group probes as powerful reporters of protein structure and dynamics.

**Acknowledgment.** A.J.B., T.L.R., and G.B. acknowledge the European Molecular Biology Organization and the Canadian Institutes of Health Research (CHIR) for postdoctoral fellowships. D.F.H. is supported by a postdoctoral fellowship from the CIHR. This work was supported by a grant from the CIHR. L.E.K. holds a Canada Research Chair in Biochemistry.

**Supporting Information Available:** Details of protein expression, experimental measurements and calculation of  $R_{2,1} - R_{2,A}$  from measured <sup>13</sup>C  $T_1$  values. This material is available free of charge via the Internet at <http://pubs.acs.org>.

## References

- Ruschak, A. M.; Kay, L. E. *J. Biomol. NMR* **2010**, *46*, 75–87.
- Tugarinov, V.; Kay, L. E. *ChemBioChem* **2005**, *6*, 1567–77.
- Gelis, I.; Bonvin, A. M.; Keramisanou, D.; Koukaki, M.; Gouridis, G.; Karamanou, S.; Economou, A.; Kalodimos, C. G. *Cell* **2007**, *131*, 756–69.
- Kay, L. E.; Torchia, D. A. *J. Magn. Reson.* **1991**, *95*, 536–547.
- Tugarinov, V.; Hwang, P.; Ollerenshaw, J.; Kay, L. E. *J. Am. Chem. Soc.* **2003**, *125*, 10420–10428.
- Sprangers, R.; Kay, L. E. *Nature* **2007**, *445*, 618–22.
- Amero, C.; Schanda, P.; Dura, M. A.; Ayala, I.; Marion, D.; Franzetti, B.; Brutscher, B.; Boisbouvier, J. *J. Am. Chem. Soc.* **2009**, *131*, 3448–9.
- Kreishman-Deitrick, M.; Goley, E. D.; Burdine, L.; Denison, C.; Egile, C.; Li, R.; Murali, N.; Kodadek, T. J.; Welch, M. D.; Rosen, M. K. *Biochemistry* **2005**, *44*, 15247–56.
- Palmer, A. G.; Kroenke, C. D.; Loria, J. P. *Methods Enzymol.* **2001**, *339*, 204–238.
- Korzhnev, D. M.; Mittermaier, A. K.; Kay, L. E. *J. Biomol. NMR* **2005**, *31*, 337–42.
- Tugarinov, V.; Kay, L. E. *J. Am. Chem. Soc.* **2007**, *129*, 9514–21.
- Religa, T. L.; Kay, L. E. *J. Biomol. NMR* **2010**, *47*, 163–169.
- Vallurupalli, P.; Hansen, D. F.; Stollar, E. J.; Meirovitch, E.; Kay, L. E. *Proc. Natl. Acad. Sci. U.S.A.* **2007**, *104*, 18473–18477.
- Mulder, F. A. A.; Skrynnikov, N. R.; Hon, B.; Dahlquist, F. W.; Kay, L. E. *J. Am. Chem. Soc.* **2001**, *123*, 967–975.
- Hansen, D. F.; Vallurupalli, P.; Kay, L. E. *J. Phys. Chem.* **2008**, *112*, 5898–5904.
- Cavanagh, J.; Rance, M. *Ann. Rep. NMR Spectrosc.* **1993**, *27*, 1–58.
- Kay, L. E.; Keifer, P.; Saarinen, T. *J. Am. Chem. Soc.* **1992**, *114*, 10663–10665.
- Schleucher, J.; Schwendinger, M.; Sattler, M.; Schmidt, P.; Schedletzky, O.; Glaser, S. J.; Sorensen, O. W.; Griesinger, C. *J. Biomol. NMR* **1994**, *4*, 301–306.
- Madi, Z. L.; Brutscher, B.; Schulteherbruggen, T.; Bruschweiler, R.; Ernst, R. R. *Chem. Phys. Lett.* **1997**, *268*, 300–305.
- Loria, J. P.; Rance, M.; Palmer, A. G. *J. Am. Chem. Soc.* **1999**, *121*, 2331–2332.
- Palmer, A. G.; Skelton, N. J.; Chazin, W. J.; Wright, P. E.; Rance, M. *Mol. Phys.* **1992**, *75*, 699–711.
- Cavanagh, J.; Fairbrother, W. J.; Palmer, A. G.; Skelton, N. J. *Protein NMR Spectroscopy: Principles and Practice*; Academic Press: San Diego, 1996.
- Baldwin, A. J.; Hansen, D. F.; Vallurupalli, P.; Kay, L. E. *J. Am. Chem. Soc.* **2009**, *131*, 11939–48.
- Sprangers, R.; Li, X.; Mao, X.; Rubinstein, J. L.; Schimmer, A. D.; Kay, L. E. *Biochemistry* **2008**, *47*, 6727–34.
- Religa, T. L.; Sprangers, R.; Kay, L. E. *Science* **2010**, *328*, 98–102.
- Lundstrom, P.; Vallurupalli, P.; Religa, T. L.; Dahlquist, F. W.; Kay, L. E. *J. Biomol. NMR* **2007**, *38*, 79–88.
- Shaka, A. J.; Lee, C. J.; Pines, A. *J. Magn. Reson.* **1988**, *77*, 274.
- Shaka, A. J.; Keeler, J.; Frenkiel, T.; Freeman, R. *J. Magn. Reson.* **1983**, *52*, 335–338.
- Skrynnikov, N. R.; Dahlquist, F. W.; Kay, L. E. *J. Am. Chem. Soc.* **2002**, *124*, 12352–60.
- Lowe, J.; Stock, D.; Jap, B.; Zwickl, P.; Baumeister, W.; Huber, R. *Science* **1995**, *268*, 533–9.

JA104578N